PCCP

Accepted Manuscript

This article can be cited before page numbers have been issued, to do this please use: X. Jiang, Y. Xu, X. Wang, Y. Wu, G. Feng, C. Li, W. Ma and W. Li, *Phys. Chem. Chem. Phys.*, 2017, DOI: 10.1039/C7CP00494J.

ROYAL SOCIETY OF CHEMISTRY

rsc.li/pccp

View Article Online
DOI: 10.1039/C7CP00494J

Journal Name

ARTICLE

Non-Fullerene Organic Solar Cells based on Diketopyrrolopyrrole Polymers as Electron Donor and ITIC as Electron Acceptor

Received 00th January 20xx,
Accepted 00th January 20xx

DOI: 10.1039/x0xx00000x

www.rsc.org/

Xudong Jiang,[ab] Yunhua Xu,*[a] Xiaohui Wang,[c] Yang Wu,[c] Guitao Feng,[ab] Cheng Li,[b] Wei Ma*[c] and Weiwei Li*[b]

In this work, we provide systemmatically studies on the non-fullerene solar cells based on diketopyrrolopyrrole (DPP) polymers as electron donor and a well-known electron acceptor ITIC. ITIC has been widely reported in non-fullerene solar cells with high power conversion efficiencies (PCEs) above 10% when combining with wide band gap conjugated polymer, while its application in small band gap DPP polymers has never been reported. Herein, we select four DPP polymers containing different thienyl linkers, resulting in distinct absorption spectra, energy levels and crystalline properties. Non-fullerene solar cells based on DPP polymers as donor and ITIC as acceptor show PCEs of 1.9% - 4.1% and energy loss of 0.55 – 0.82 eV. The PCEs are much lower than those of cells based on fullerene derivatives due to the poor miscibility between the DPP polymers and ITIC, as confirmed by the morphology and charge transport invesgitation. The results indicate that it is important to tune the miscibility between donor and acceptor in order to realize optimzed micro-phase separation, which can further enhance the performance of DPP polymers based non-fullerene solar cells.

Introduction

Organic solar cells have entered a new era of non-fullerene electron acceptors, as evidenced by the fast development of non-fullerene organic solar cells (NFOSCs) in recent years with power conversion efficiencies (PCEs) above 12%.[1-5] Intensive modification of the chemical structures enables non-fullerene conjugated materials to desire tunable energy levels, charge transport and crystal properties in order to meet the requirement of electron donors, providing the opportunity to improve the photovoltaic performance.[6-16] It has been reported that when lowering the energy loss (E_{loss}) defined as the difference between the optical band gap (E_g) and open-circuit voltage (V_{oc}), and realizing high external quantum efficiencies (EQE),[17] the PCEs of NFOSCs can be close to 20%.[18] NFOSCs also show good thermal and bending stability, indicating their promising application in large-area devices.[19]

Nowadays, the most successful strategies to achieve high performance NFOSCs are to use two components with complementary absorption spectra in photo-active layers, such as wide band gap (with absorption onset below 700 nm) and medium band gap (with absorption onset around 800 nm) conjugated materials. For instance, perylene bisimide (PBI) based electron acceptors with strong absorption at 400 – 600 nm can show PCEs above 9% when combining with low band gap conjugated polymers as donor.[20] The other electron acceptors are developed by using electron-donating centre and electron-withdrawing end groups, such as the molecules reported by McCulloch et al.[3, 21, 22] and Zhan et al.[7, 23-25] with the absorption extending to near-infrared region. These low band gap electron acceptors were applied into high performance NFOSCs by using wide band gap polymers as electron donor. Among them, a non-fullerene molecule, 3,9-bis(2-methylene-(3-(1,1-dicyanomethylene)-indanone)-5,5,11,11-tetrakis(4-hexylphenyl) -dithieno[2,3-*d*:2′,3′-*d*′]-*s*-indaceno[1,2-*b*:5,6-*b*′]dithiophene (ITIC) with absorption onset close to 800 nm, has been widely reported as an universal electron acceptor in NFOSCs.[1, 25-31]

Since sunlight covers broad spectrum from 300 nm to 1000 nm, it is important to develop NFOSCs with photo-response in the region. This has also been reported in the literatures, especially with photo-response above 900 nm, but the PCEs were below 4%.[32-34] This is mainly due to the limited materials selection of the ultra-low band gap polymers, mainly based on diketopyrrolopyrrole (DPP) units. Therefore, it is still a challenging task to study the NFOSCs with photo-response up to 1000 nm in order to sufficiently utilize the solar energy and also be applied into tandem and triple-junction solar cells.[35]

In this work, we are working on NFOSCs based on DPP polymers as electron donor and ITIC as electron acceptor, which has not been reported elsewhere. DPP polymers have shown successful application in fullerene-based solar cells, such as using [6,6]-phenyl-C71-butyric acid methyl ester ([70]PCBM) as acceptor with PCE above 9%.[36, 37] However, the

[a] Department of Chemistry, School of Science, Beijing Jiaotong University, Beijing 100044, P. R. China. E-mail: yhxu@bjtu.edu.cn.
[b] Beijing National Laboratory for Molecular Sciences, CAS Key Laboratory of Organic Solids, Institute of Chemistry, Chinese Academy of Sciences, Beijing 100190, P. R. China. E-mail: liweiwei@iccas.ac.cn.
[c] State Key Laboratory for Mechanical Behavior of Materials, Xi'an Jiaotong University, Xi'an 710049, P. R. China. E-mail: msewma@xjtu.edu.cn.

View Article Online
DOI: 10.1039/C7CP00494J

performance of NFOSCs based on DPP polymer donors is out of expectation, although DPP polymers were reported to show narrow band gap, high hole mobilities[38] and good crystallinity.[39] In our previous work, we applied several electron acceptors into DPP polymer solar cells, but EQE is below 0.3 compared to EQE of 0.65 when using PCBM as acceptor (Fig. 1).[16, 33, 34, 40] Herein, we apply ITIC into DPP polymer solar cells, resulting in a highest PCE of 4.1% with EQE above 0.4. We further study the morphology and charge transport properties in bulk-heterojunction (BHJ) thin films, in which we found that the hole mobilities and crystallinity of DPP polymers in blended thin films were similar with those in pure polymer films. Therefore, we speculate that DPP polymers have poor miscibility with ITIC, resulting in poor phase separation with large domain and hence relatively low PCEs in solar cells.

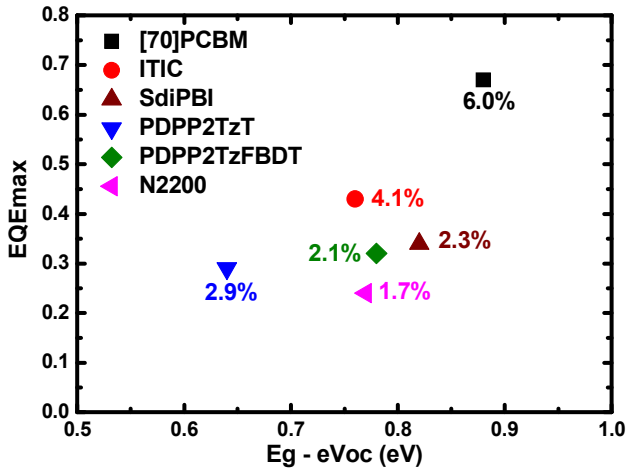

Fig. 1 Maximum EQE vs the energy loss (E_g – eV_{oc}) for PDPP5T based fullerene and non-fullerene solar cells. PCBM: Ref. 16. SdiPBI: Ref. 33. PDPP2TzT: Ref. 16. PDPP2TzFBDT: Ref. 40. Ref: N2200: Ref. 34. ITIC: this work.

Experimental

Commercial chemicals (from Sigma-Aldrich, JK Chemical and TCI) were used as received. DPP polymers, PDPP3T,[41] PDPP4T,[39] PDPP5T,[42] PDPP6T[42] and ITIC[7] were synthesized according to the literatures. Molecular weight was determined with gel permeation chromatography (GPC) at 140 °C on a PL-GPC 220 system (Agilent Technologies with a Knauer PDA detector) using a PLgel 10µm MIXED-B LS column and *o*-DCB as the eluent against polystyrene standards. Low concentration of 0.1 mg mL^{-1} polymer in *o*-DCB was applied to reduce aggregation. The molecule weight (M_p) for these polymers is 369 kg mol^{-1} (PDPP3T), 156 kg mol^{-1} (PDPP4T), 42 kg mol^{-1} (PDPP5T) and 34 kg mol^{-1} (PDPP6T). Optical absorption spectra were recorded on a JASCO V-570 spectrometer with a slit width of 2.0 nm and a scan speed of 1000 nm min^{-1}. Cyclic voltammetry was performed under an inert atmosphere at a scan rate of 0.1 V s^{-1} and 1 M tetrabutylammoniumhexafluorophosphate in acetonitrile as the electrolyte, a glassy-carbon working electrode coated with samples, a platinum-wire auxiliary electrode, and an Ag/AgCl as a reference electrode.

Atomic force microscopy (AFM) images were recorded using a Digital Instruments Nano scope IIIa multimode atomic force microscope in tapping mode under ambient conditions. Steady state fluorescence spectra were recorded at room temperature using an Edinburgh Instruments FLS980 double-monochromator luminescence spectrometer equipped with a nitrogen-cooled near-IR sensitive photomultiplier (Hamamatsu).

2D-GIWAXS measurements were performed at beamline 7.3.3[43] at the Advanced Light Source. Samples were prepared on Si substrates using identical blend solutions as those used in devices. The 10 keV X-ray beam was incident at a grazing angle of 0.12°-0.16°, selected to maximize the scattering intensity from the samples. The scattered x-rays were detected using a Dectris Pilatus 2M photon counting detector.

R-SoXS transmission measurements were performed at beamline 11.0.1.2[44] at the Advanced Light Source (ALS). Samples for R-SoXS measurements were prepared on a PEDOT:PSS modified Si substrate under the same conditions as those used for device fabrication, and then transferred by floating in water to a 1.5 mm × 1.5 mm, 100 nm thick Si_3N_4 membrane supported by a 5 mm × 5 mm, 200 µm thick Si frame (Norcada Inc.). 2-D scattering patterns were collected on an in-vacuum CCD camera (Princeton Instrument PI-MTE). The sample detector distance was calibrated from diffraction peaks of a triblock copolymer poly(isoprene-*b*-styrene-*b*-2-vinyl pyridine), which has a known spacing of 391 Å. The beam size at the sample is approximately 100 µm by 200 µm.

Photovoltaic devices with inverted configuration were made by spin-coating a ZnO sol-gel[45] at 4000 rpm for 60 s onto pre-cleaned, patterned ITO substrates. The photoactive layer was deposited by spin coating a $CHCl_3$ solution containing DPP polymers and ITIC and the appropriate amount of DIO as processing additive in air. MoO_3 (10 nm) and Ag (100 nm) were deposited by vacuum evaporation at ca. 4 × 10^{-5} Pa as the back electrode.

The active area of the cells was 0.04 cm^2. The *J-V* characteristics were measured by a Keithley 2400 source meter unit under AM1.5G spectrum from a solar simulator (Enlitech model SS-F5-3A). Solar simulator illumination intensity was determined at 100 mW cm^{-2} using a monocrystal silicon reference cell with KG5 filter. Short circuit currents under AM1.5G conditions were estimated from the spectral response and convolution with the solar spectrum. The external quantum efficiency was measured by a Solar Cell Spectral Response Measurement System QE-R3011 (Enli Technology Co., Ltd.). The thickness of the active layers in the photovoltaic devices was measured on a Veeco Dektak XT profilometer.

Results and discussion

Absorption and energy levels

View Article Online
DOI: 10.1039/C7CP00494J

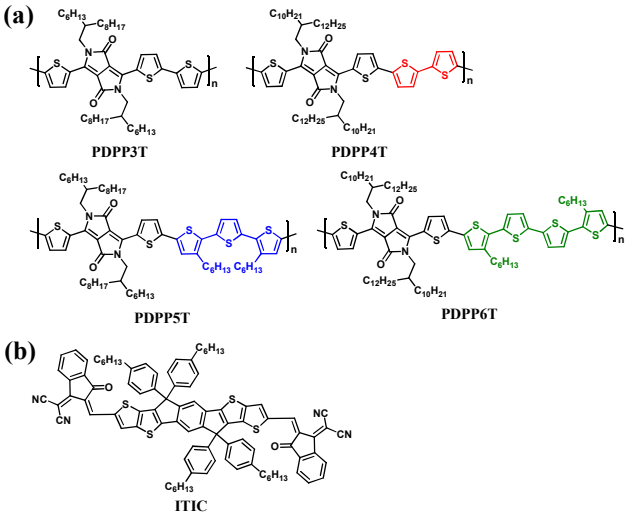

Fig. 2 The chemical structures of (a) DPP polymers as electron donor and (b) the electron acceptor ITIC.

The chemical structures of the DPP polymers and ITIC were shown in Fig. 2. We select four DPP polymers containing DPP core alternating with oligothiophenes, as PDPP3T, PDPP4T, PDPP5T and PDPP6T (Fig. 2). These DPP polymers were synthesized in our lab according to the literatures, by using the Stille polymerization condition of a catalyst system of $Pd_2(dba)_3/PPh_3$ and the solvent mixure toluene/DMF. When the number of thiophene segments was increased, the absorption of the DPP polymers was blue-shifted (Fig. 3a). Therefore, the optical band gap is increased from 1.33 eV to 1.43 eV, 1.45 eV and 1.50 eV for PDPP3T – PDPP6T (Table 1). Absorption spectrum of ITIC in thin film was also listed in Fig. 3a, showing absorption onset at 780 nm with E_g of 1.59 eV.

Energy levels of the DPP polymers and ITIC were determined by cylic voltammetry (CV) measurement in thin films, as shown in Fig. 3b and summarized at Table 1. Highest occupied molecular orbital (HOMO) levels of these conjugated materials were calculated from the onset of oxidation potential, showing that the HOMO levels are gradually shifted to high-lying position, from -5.40 eV for PDPP3T, to -5.25 – 5.33 eV for the other DPP polymers (Table 1). Similar trends can also be found in the lowest unoccupied molecular orbital (LUMO) levels of the DPP polymers, providing LUMO levels of -3.80 eV - -4.07 eV. HOMO and LUMO level of ITIC determined under the same measurement condition are -5.61 eV and -4.02 eV. Therefore, we can calculate the HOMO and LUMO difference between the donor polymers and ITIC (ΔE_{HOMO} and ΔE_{LUMO}). HOMO offset is around 0.20 – 0.36 eV, while LUMO offset has significantly difference. Interestingly, LUMO offset between PDPP3T and ITIC is even negative, indicating the negligible driving force for exciton dissociation into free charges. The small LUMO offset will influence the charge separation process in organic photovoltaic cells due to the low driving force for exciton dissociation into free charges.

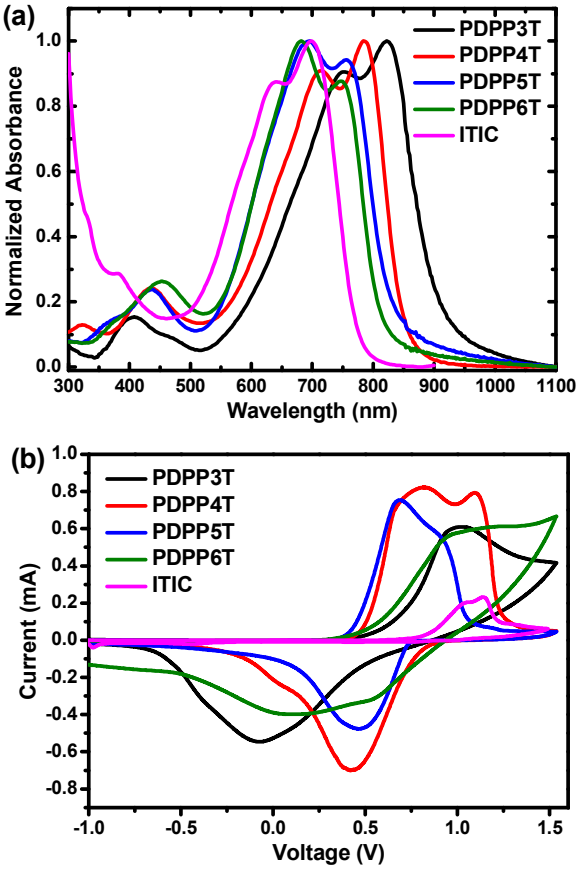

Fig. 3 (a) Absorption spectra of pure DPP polymers and ITIC thin films. (b) Cyclic voltammogram of the DPP polymers and ITIC thin films. Potential vs. F_c/F_c^+.

Table 1. Optical and Electrochemical Properties of the DPP polymers and ITIC.

Polymer	λ_{onset} (nm)	E_g^{film} (eV)	E_{HOMO} [a] (eV)	E_{LUMO} [b] (eV)	ΔE_{HOMO} [c] (eV)	ΔE_{LUMO} [d] (eV)
PDPP3T	932	1.33	-5.40	-4.07	0.21	-0.05
PDPP4T	867	1.43	-5.30	-3.87	0.31	0.15
PDPP5T	855	1.45	-5.25	-3.80	0.36	0.22
PDPP6T	826	1.50	-5.33	-3.83	0.28	0.19
ITIC	780	1.59	-5.61	-4.02	-	-

[a] Determined using a work function value of -4.8 eV for Fc/Fc^+. [b] Determined as $E_{HOMO} + E_g^{film}$. [c] $\Delta E_{HOMO} = E_{HOMO}$ (polymer) – E_{HOMO} (ITIC). [d] $\Delta E_{LUMO} = E_{LUMO}$ (polymer) – E_{LUMO} (ITIC).

Non-fullerene solar cells

Non-fullerene solar cells were fabricated by using DPP polymers as electron donor and ITIC as electron acceptor. The photovoltaic devices were using inverted configuration with ITO/ZnO and MoO_3/Ag as electrode. The photo-active layers were solution-processed from $CHCl_3$, in which the high boiling point additive, ratio of donor to acceptor and thickness were carefully optimized, as summarized in the Supporting Information (Table S1 – S4). In general, PDPP3T and PDPP4T based cells provided the optimized performance with the ratio of donor to acceptor of 1:2 under fabrication condition of $CHCl_3$ with 0.2% DIO, while PDPP5T and PDPP6T have the best

View Article Online
DOI: 10.1039/C7CP00494J

performance with the ratio of 1:1.5. The optimized *J-V* characteristics were shown in Fig. 4a and the photovoltaic parameters were summarized at Table 2.

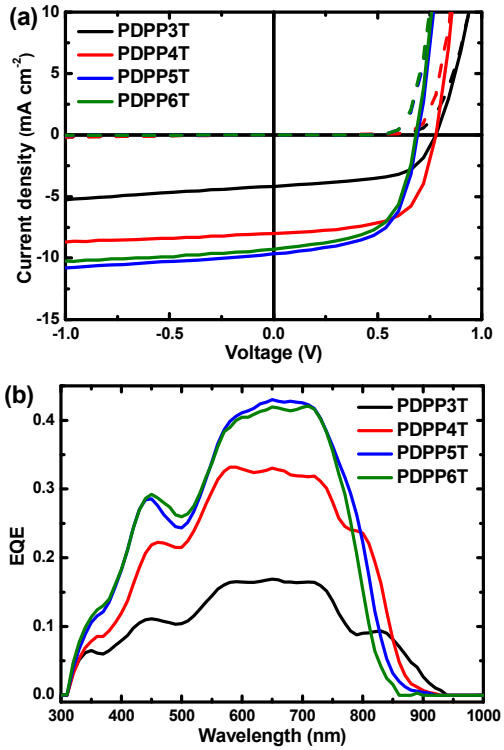

Fig. 4 (a) *J-V* characteristics in the dark (dashed lines) and under white light illumination (solid lines). (b) EQE of the optimized DPP polymer:ITIC solar cells.

Table 2. Solar cell parameters of optimized solar cells of DPP-polymer:ITIC

Polymer	J_{sc}[c] (mA cm^{-2})	V_{oc} (V)	FF	PCE (%)	E_{loss} (eV)
PDPP3T[a]	4.2	0.78	0.59	1.9	0.55
PDPP4T[a]	8.0	0.78	0.63	3.9	0.65
PDPP5T[b]	9.6	0.69	0.61	4.1	0.76
PDPP6T[b]	9.3	0.68	0.60	3.8	0.82

[a]Ratio of donor to acceptor is 1:2. [b]Ratio of donor to acceptor is 1:1.5. Optimized spin coating solvent for active layer is $CHCl_3$ with 0.2% DIO as additive. [c]J_{sc} as calculated by integrating the EQE spectrum with the AM1.5G spectrum. The thickness of active layers is 70 – 80 nm.

PDPP3T:ITIC cells show the best PCE of 1.9% with a short-circuit current density (J_{sc}) of 4.2 mA cm^{-2}, V_{oc} of 0.78 V and fill factor (FF) of 0.59. The PCE was significantly enhanced to 3.9% for PDPP4T:ITIC cells, which is mainly attributed to higher J_{sc} of 8.0 mA cm^{-2} and FF of 0.63. The J_{sc} of PDPP5T:ITIC cells was further increased to 9.6 mA cm^{-2}, but with reduced V_{oc} of 0.69 V, so the PCE is slightly increased to 4.1%. To the best of our knowledge, this also presents the best non-fullerene solar cells based on DPP polymers as electron donor. The PCE of PDPP6T:ITIC was slightly drop to 3.8% due to decreased J_{sc} of 9.3 mA cm^{-2}. The J_{sc}s of these cells were also reflected by their EQEs, as shown in Fig. 4b. PDPP3T:ITIC cells perform broad photo-response from 300 nm to 900 nm, but the EQE is below 0.2. EQE can be further enhanced to 0.3 for PDPP4T:ITIC cells and 0.4 for PDPP5T and PDPP6T based cells. EQE above 0.4 also represent the highest EQE in DPP polymers based non-fullerene solar cells, confirming that ITIC is an universal electron acceptor.[25] The trend of EQE enhancement from PDPP3T to PDPP6T can be due to the gradually enhanced E_{loss} from 0.55 eV to 0.82 eV, as shown in Table 2. We speculate that in DPP polymers, high E_{loss} is important for efficient charge separation in BHJ system.[42] This can be further confirmed by steady-state photoluminescence (PL) measurement, as shown in Fig. 5. The PL of PDPP3T in blended thin films was not quenched, while PDPP4T showed obviously quenched PL spectra in blended thin films. Quenching ratio can further increase for PDPP5T and PDPP6T based blended thin films (Fig. 5). It is assumed that when LUMO or HOMO difference between donor and acceptor is small, the charge separation will be insufficient, causing poor PL quenching. This can explain the low EQE and J_{sc} in PDPP3T and PDPP4T cells.

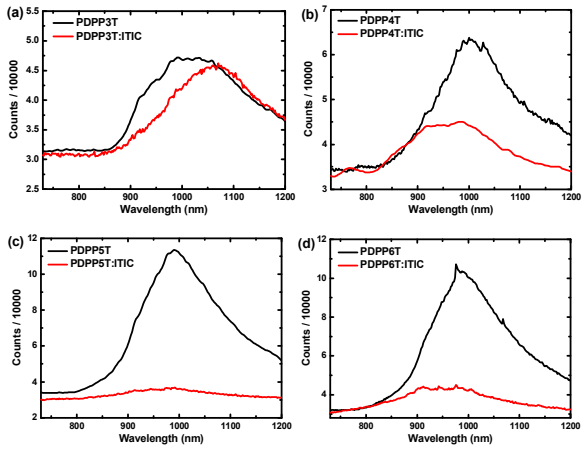

Fig. 5 Photoluminescence spectra of the DPP polymers and the blends of DPP polymer:ITIC. The fabrication condition is indicated in Table 2. The thin films were excited at 710 nm for measurements.

Morphology investigation

EQE and J_{sc} of these cells are still low compared to PCBM based cells, as indicated in Fig. 1. Therefore, we intend to provide deep insight into the morphology and charge transport properties in these systems. We firstly apply atomic force microscopy (AFM) to analysis the morphology of blended thin films, as shown in Fig. 6. At first glance, all the thin films present smooth surface as indicated by the small roughness (1.3 – 1.7 nm). However, we can observe worm-like structures or crystallized domain in these thin films. These structures were possibly attributed to the crystallize DPP polymers, indicating the DPP polymers and ITIC have large phase separation with poor miscibility.

View Article Online
DOI: 10.1039/C7CP00494J

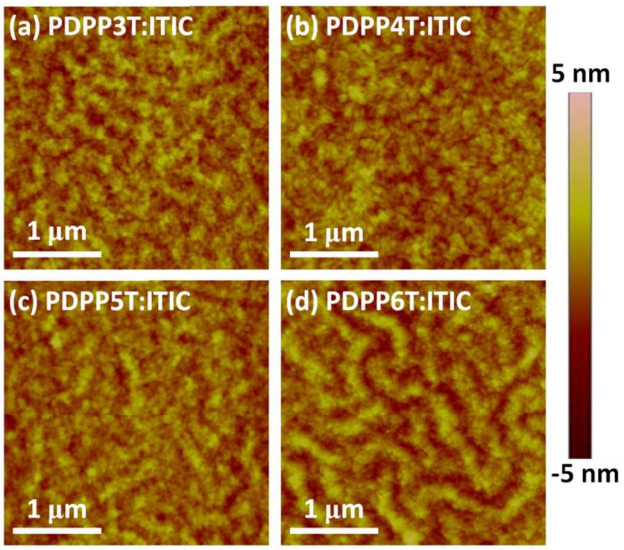

Fig. 6 AFM height images (3 × 3 μm^2) of optimized DPP polymer:ITIC active layers spin coated from chloroform containing 0.2% DIO. (a) PDPP3T, (b) PDPP4T, (c) PDPP5T and (d) PDPP6T.The root mean square (RMS) roughness values for (a – d) is 1.4 nm, 1.4 nm, 1.3 nm and 1.7 nm.

This can be further confirmed by 2D grazing-incidence wide-angle X-ray scattering (2D-GIWAXS) measurement, as shown in Fig. 7. These DPP polymers present good crystal properties, as revealed by their high ordering reflection patterns of (*h*00) peaks and (010) diffraction peaks (Fig. 7a-d). When blended with ITIC, the crystallinity of DPP polymers is slightly reduced, but the diffraction patterns are similar to those of pure polymers. The results indicate that incorporation of ITIC into DPP polymers has little impact on the crystallization of DPP polymers. We further use R-SoXS to get the information regarding the characteristic mode length (domain size) as shown in Fig. S1 and Table S5, in which large domain size is correlated to the better phase separation and high FF. The blended thin films based on these DPP polymers have domain size of 23 – 31 nm, explaining their similar FF in solar cells.

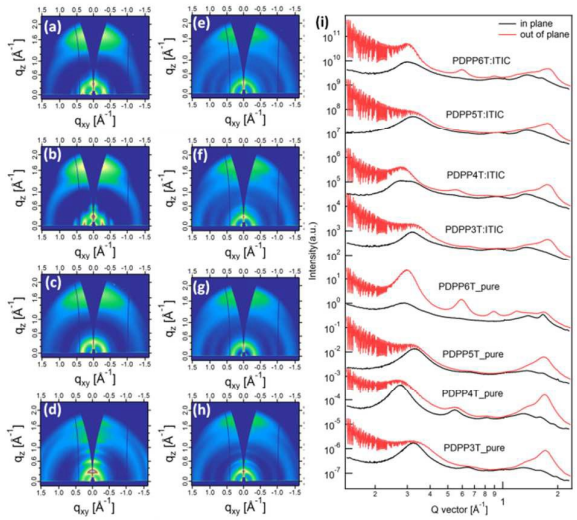

Fig. 7 2D-GIWAXS images of the pure DPP polymer thin films and blends fabricated from CHCl3 with 0.2% DIO. (a-d) pure polymers. (e-h) blends of DPP polymer:ITIC. (i) the OOP and IP cuts of the corresponding 2D-GIWAXS patterns.

Charge carrier investigation

We further applied space-charge limit current (SCLC) measurement to study the charge transport properties of the pure DPP polymers and blended thin films, as shown in Fig. 8 and Table 3. The pure DPP polymers exhibit hole mobility between 1.2 × 10^{-4} cm^2 V^{-1} s^{-1} and 4.8 × 10^{-4} cm^2 V^{-1} s^{-1}. The hole mobility in blended thin films is slightly increased, but very similar to those of pure polymers. As observed in AFM and 2D-GIWAXS, the crystallization of DPP polymers is not disturbed in blended thin films, which shows similar charge transport channel for charge transport. Thus, this explains the similar charge mobility of DPP polymers in pure and blended thin films.

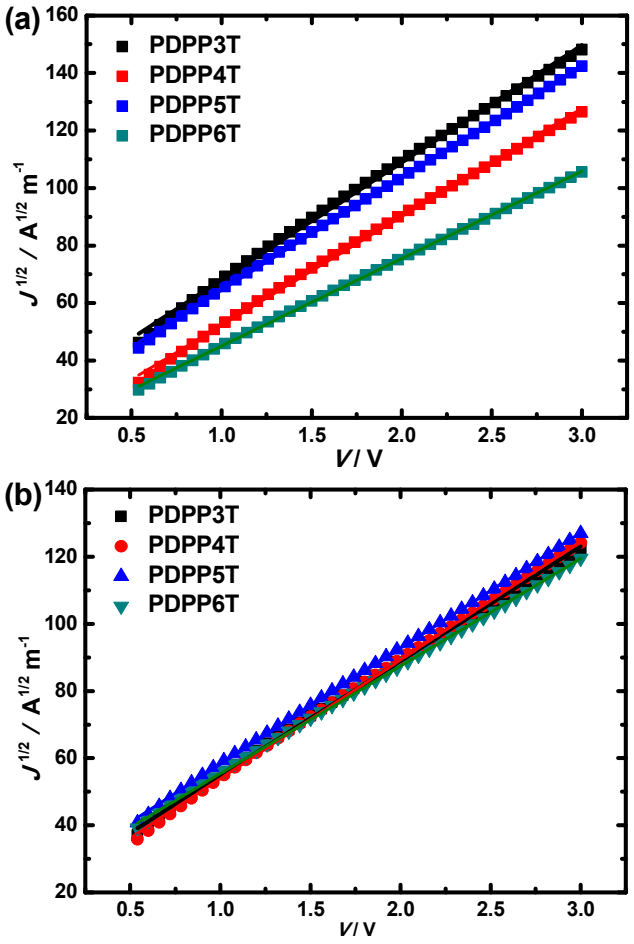

Fig. 8 *J-V* characteristics under dark for hole-only devices. (a) pure DPP polymers. (b) DPP polymer blended with ITIC. The device structure is ITO/PEDOT:PSS/organic thin film/MoO_3/Ag.

View Article Online
DOI: 10.1039/C7CP00494J

Table 3. Solar cell parameters of optimized solar cells of DPP polymer:ITIC

	μ_h (pure) [a] ($cm^2 V^{-1} s^{-1}$)	μ_h (blend) [b] ($cm^2 V^{-1} s^{-1}$)
PDPP3T	2.2×10^{-4}	2.8×10^{-4}
PDPP4T	4.8×10^{-4}	7.2×10^{-4}
PDPP5T	1.6×10^{-4}	3.8×10^{-4}
PDPP6T	1.2×10^{-4}	2.2×10^{-4}

[a]pure DPP polymers. [b]DPP polymers blended with ITIC. The fabrication condition is shown in Table 2.

Conclusions

In this work, we study the non-fullerene solar cells based on DPP polymers and ITIC, and explore the limitation in these cells. We achieve PCEs up to 4% in solar cells, with the photo-response from 300 nm to 900 nm. This is also one of the best PCEs in DPP polymers based non-fullerene solar cells. Morphology investigation by AFM and 2D-GIWAXS reveals that DPP polymers and ITIC have poor miscibility, causing large phase separation in bulk-heterojunction thin films, reducing photocurrent and PCEs. This can be further confirmed by SCLC measurement, in which the hole mobility in pure and blended thin films is quite similar. These results show that tuning the micro-phase separation by chemical and physical method, especially focusing on improving the miscibility of the DPP polymers and ITIC, will be beneficial for high performance non-fullerene solar cells based on DPP polymers as electron donor owing to their broad absorption spectra.

Acknowledgements

We thank Prof. Yi Zhou and Prof. Yongfang Li at Soochow University for steady state PL measurement. This work was supported by the Recruitment Program of Global Youth Experts of China. The work was further supported by the National Natural Science Foundation (NSFC) of China (21574138, 51603209, 91427303) and the Strategic Priority Research Program (XDB12030200) of the Chinese Academy of Sciences. Wei Ma thanks for the support from Ministry of science and technology (No. 2016YFA0200700), NSFC (21504066, 21534003). X-ray data was acquired at beamlines 7.3.3 and 11.0.1.2 at the Advanced Light Source, which is supported by the Director, Office of Science, Office of Basic Energy Sciences, of the U.S. Department of Energy under Contract No. DE-AC02-05CH11231. The authors thank Chenhui Zhu at beamline 7.3.3, and Cheng Wang at beamline 11.0.1.2 for assistance with data acquisition.

Notes and references

1. S. Li, L. Ye, W. Zhao, S. Zhang, S. Mukherjee, H. Ade and J. Hou, *Adv. Mater.*, 2016, **28**, 9423-9429.
2. Y. Lin and X. Zhan, *Acc. Chem. Res.*, 2016, **49**, 175-183.
3. C. B. Nielsen, S. Holliday, H.-Y. Chen, S. J. Cryer and I. McCulloch, *Acc. Chem. Res.*, 2015, **48**, 2803-2812.
4. C. Zhan and J. Yao, *Chem. Mater.*, 2016, **28**, 1948-1964.
5. H. Benten, D. Mori, H. Ohkita and S. Ito, *J. Mater. Chem. A*, 2016, **4**, 5340-5365.
6. A. Kuzmich, D. Padula, H. Ma and A. Troisi, *Energy Environ. Sci.*, 2017, DOI: 10.1039/C1036EE03654F.
7. Y. Lin, J. Wang, Z.-G. Zhang, H. Bai, Y. Li, D. Zhu and X. Zhan, *Adv. Mater.*, 2015, **27**, 1170-1174.
8. W. Jiang, L. Ye, X. Li, C. Xiao, F. Tan, W. Zhao, J. Hou and Z. Wang, *Chem. Commun.*, 2014, **50**, 1024-1026.
9. O. K. Kwon, J.-H. Park, S. K. Park and S. Y. Park, *Adv. Energy Mater.*, 2015, **5**, 1400929.
10. Z. H. Mao, W. Senevirathna, J. Y. Liao, J. Gu, S. V. Kesava, C. H. Guo, E. D. Gomez and G. Sauve, *Adv. Mater.*, 2014, **26**, 6290-6294.
11. J. Zhang, H. Xiao, X. Zhang, Y. Wu, G. Li, C. Li, X. Chen, W. Ma and Z. Bo, *J. Mater. Chem. C*, 2016, **4**, 5656-5663.
12. C. Duan, G. Zango, M. García Iglesias, F. J. M. Colberts, M. M. Wienk, M. V. Martínez-Díaz, R. A. J. Janssen and T. Torres, *Angew. Chem., Int. Ed.*, 2017, **56**, 148-152.
13. S. Li, W. Liu, M. Shi, J. Mai, T.-K. Lau, J. Wan, X. Lu, C.-Z. Li and H. Chen, *Energy Environ. Sci.*, 2016, **9**, 604-610.
14. L. Gao, Z.-G. Zhang, L. Xue, J. Min, J. Zhang, Z. Wei and Y. Li, *Adv. Mater.*, 2016, **28**, 1884-1890.
15. A. Facchetti, *Mater Today*, 2013, **16**, 123-132.
16. W. Li, W. S. C. Roelofs, M. Turbiez, M. M. Wienk and R. A. J. Janssen, *Adv. Mater.*, 2014, **26**, 3304-3309.
17. W. Li, K. H. Hendriks, A. Furlan, M. M. Wienk and R. A. J. Janssen, *J. Am. Chem. Soc.*, 2015, **137**, 2231-2234.
18. D. Baran, T. Kirchartz, S. Wheeler, S. Dimitrov, M. Abdelsamie, J. Gorman, R. S. Ashraf, S. Holliday, A. Wadsworth, N. Gasparini, P. Kaienburg, H. Yan, A. Amassian, C. J. Brabec, J. R. Durrant and I. McCulloch, *Energy Environ. Sci.*, 2016, **9**, 3783-3793.
19. T. Kim, J.-H. Kim, T. E. Kang, C. Lee, H. Kang, M. Shin, C. Wang, B. Ma, U. Jeong, T.-S. Kim and B. J. Kim, *Nat. Commun.*, 2015, **6**, 8547.
20. J. Liu, S. Chen, D. Qian, B. Gautam, G. Yang, J. Zhao, J. Bergqvist, F. Zhang, W. Ma, H. Ade, O. Inganäs, K. Gundogdu, F. Gao and H. Yan, *Nat. Energy*, 2016, **1**, 16089.
21. D. Baran, R. S. Ashraf, D. A. Hanifi, M. Abdelsamie, N. Gasparini, J. A. Rohr, S. Holliday, A. Wadsworth, S. Lockett, M. Neophytou, C. J. M. Emmott, J. Nelson, C. J. Brabec, A. Amassian, A. Salleo, T. Kirchartz, J. R. Durrant and I. McCulloch, *Nat. Mater.*, 2016, **doi:10.1038/nmat4797**, doi:10.1038/nmat4797.
22. S. Holliday, R. S. Ashraf, A. Wadsworth, D. Baran, S. A. Yousaf, C. B. Nielsen, C.-H. Tan, S. D. Dimitrov, Z. Shang, N. Gasparini, M. Alamoudi, F. Laquai, C. J. Brabec, A. Salleo, J. R. Durrant and I. McCulloch, *Nat. Commun.*, 2016, **7**, 11585.
23. Y. Lin, Q. He, F. Zhao, L. Huo, J. Mai, X. Lu, C.-J. Su, T. Li, J. Wang, J. Zhu, Y. Sun, C. Wang and X. Zhan, *J. Am. Chem. Soc.*, 2016, **138**, 2973-2976.
24. Y. Lin, F. Zhao, Q. He, L. Huo, Y. Wu, T. C. Parker, W. Ma, Y. Sun, C. Wang, D. Zhu, A. J. Heeger, S. R. Marder and X. Zhan, *J. Am. Chem. Soc.*, 2016, **138**, 4955-4961.
25. Y. Lin, F. Zhao, Y. Wu, K. Chen, Y. Xia, G. Li, S. K. K. Prasad, J. Zhu, L. Huo, H. Bin, Z.-G. Zhang, X. Guo, M. Zhang, Y. Sun, F. Gao, Z. Wei, W. Ma, C. Wang, J. Hodgkiss, Z. Bo, O. Inganäs, Y. Li and X. Zhan, *Adv. Mater.*, 2017, **29**, 1604155-n/a.
26. H. Bin, Z.-G. Zhang, L. Gao, S. Chen, L. Zhong, L. Xue, C. Yang and Y. Li, *J. Am. Chem. Soc.*, 2016, **138**, 4657-4664.

View Article Online
DOI: 10.1039/C7CP00494J

27. Y. Qin, M. A. Uddin, Y. Chen, B. Jang, K. Zhao, Z. Zheng, R. Yu, T. J. Shin, H. Y. Woo and J. Hou, *Adv. Mater.*, 2016, **28**, 9416-9422.
28. W. Zhao, D. Qian, S. Zhang, S. Li, O. Inganäs, F. Gao and J. Hou, *Adv. Mater.*, 2016, **28**, 4734-4739.
29. Y. Yang, Z.-G. Zhang, H. Bin, S. Chen, L. Gao, L. Xue, C. Yang and Y. Li, *J. Am. Chem. Soc.*, 2016, **138**, 15011-15018.
30. D. Xia, Y. Wu, Q. Wang, A. Zhang, C. Li, Y. Lin, F. J. M. Colberts, J. J. van Franeker, R. A. J. Janssen, X. Zhan, W. Hu, Z. Tang, W. Ma and W. Li, *Macromolecules*, 2016, **49**, 6445-6454.
31. H. Lu, J. Zhang, J. Chen, Q. Liu, X. Gong, S. Feng, X. Xu, W. Ma and Z. Bo, *Adv. Mater.*, 2016, **28**, 9559-9566.
32. W. Li, Y. An, M. M. Wienk and R. A. J. Janssen, *J. Mater. Chem. A*, 2015, **3**, 6756-6760.
33. C. Li, A. Zhang, G. Feng, F. Yang, X. Jiang, Y. Yu, D. Xia and W. Li, *Org. Electron.*, 2016, **35**, 112-117.
34. C. Li, A. Zhang, Z. Wang, F. Liu, Y. Zhou, T. P. Russell, Y. Li and W. Li, *RSC Adv.*, 2016, **6**, 35677-35683.
35. W. Li, A. Furlan, K. H. Hendriks, M. M. Wienk and R. A. J. Janssen, *J. Am. Chem. Soc.*, 2013, **135**, 5529-5532.
36. W. Li, K. H. Hendriks, M. M. Wienk and R. A. J. Janssen, *Acc. Chem. Res.*, 2016, **49**, 78-85.
37. Y. Liu, G. Li, Z. Zhang, L. Wu, J. Chen, X. Xu, X. Chen, W. Ma and Z. Bo, *J. Mater. Chem. A*, 2016, **4**, 13265-13270.
38. Y. Ji, C. Xiao, Q. Wang, J. Zhang, C. Li, Y. Wu, Z. Wei, X. Zhan, W. Hu, Z. Wang, R. A. J. Janssen and W. Li, *Adv. Mater.*, 2016, **28**, 943-950.
39. W. Li, K. H. Hendriks, A. Furlan, W. S. C. Roelofs, M. M. Wienk and R. A. J. Janssen, *J. Am. Chem. Soc.*, 2013, **135**, 18942-18948.
40. A. Zhang, Q. Wang, R. A. A. Bovee, C. Li, J. Zhang, Y. Zhou, Z. Wei, Y. Li, R. A. J. Janssen, Z. Wang and W. Li, *J. Mater. Chem. A*, 2016, **4**, 7736-7745.
41. K. H. Hendriks, G. H. L. Heintges, V. S. Gevaerts, M. M. Wienk and R. A. J. Janssen, *Angew. Chem., Int. Ed.*, 2013, **52**, 8341-8344.
42. W. Li, W. S. C. Roelofs, M. M. Wienk and R. A. J. Janssen, *J. Am. Chem. Soc.*, 2012, **134**, 13787-13795.
43. H. Alexander, B. Wim, G. James, S. Eric, G. Eliot, K. Rick, M. Alastair, C. Matthew, R. Bruce and P. Howard, *J. Phys. Conf. Ser.*, 2010, **247**, 012007.
44. E. Gann, A. T. Young, B. A. Collins, H. Yan, J. Nasiatka, H. A. Padmore, H. Ade, A. Hexemer and C. Wang, *Rev. Sci. Instrum.*, 2012, **83**, 045110.
45. Y. Sun, J. H. Seo, C. J. Takacs, J. Seifter and A. J. Heeger, *Adv. Mater.*, 2011, **23**, 1679-1683.